

AN EXPERIMENTAL EVALUATION OF ENGINE-DRIVEN HEAT PUMP SYSTEMS

Barry R. Maxwell
Associate Professor
Bucknell University
Lewisburg, Pa. 17837
Member

David A. Didion, Chief
Mechanical Systems Program
National Bureau of Standards
Washington, D.C. 20234
Member

ABSTRACT

A laboratory investigation was conducted of an engine-driven air-to-air, variable speed, 3-ton Rankine heat pump. A water-cooled Stirling engine was used in one series of tests and a water-cooled Diesel engine of comparable size was used in another series. The steady-state part-load performance of both engine-driven systems was determined as a function of outdoor temperature and compressor speed. Engine coolant energy and recoverable exhaust energy were determined and included in the heating mode calculations. Heating and cooling capacities, system coefficients of performance, and seasonal performance factors were determined for both systems. Additional tests were concerned with defrost mode energy requirements and the influence of coolant temperature on system performance.

NOMENCLATURE

bsfc = Brake specific fuel consumption
COP = Heat pump coefficient of performance
COP_{eff} = Coefficient of performance of engine-driven heat pump system
DD = Degree day
HP = Mechanical energy input to the compressor
HP' = Mechanical energy input to fan and miscellaneous equipment
I = Number of bins
n₁ = Number of hours in 1st temperature bin
Ne = Engine speed
N_c = Compressor speed

ODT	= Outdoor temperature
Q_F	= Engine fuel energy input
Q_H	= Heat pump heating capacity
Q_R	= Recovered waste heat energy
SPF	= Seasonal performance factor
T_i	= Median temperature of the i th bin
β	= Fraction of fuel energy recovered
η_t	= Brake thermal efficiency
α	= Parasitic power fraction

INTRODUCTION

In the last several years, increased energy costs and shortages of certain fuels have created an important and continuing need to adopt energy conservation measures throughout our society. Foremost in this area of energy conservation is the efficient heating and cooling of this nation's commercial and residential buildings. This can be partially achieved by adopting economy measures and building standards which result in lower energy consumption, and by developing more fuel efficient energy conversion systems. Included in the latter category is the heat pump.

Heat pumps are attractive building heating devices in the current economic-energy climate because of their ability to provide more output thermal energy than input energy consumed. Although the electric motor-driven Rankine cycle heat pump is the principal system currently manufactured for residential and light commercial building applications, a number of heat pump concepts employing a heat engine as a direct-drive power source have been and are being devised [1-7]. The application of a heat engine to a heat pump has the inherent advantages of engine waste heat recovery to supplement the refrigeration cycle heating mode output, and increased heat pump efficiency in both the heating and cooling modes due to capacity modulation. The effect of waste heat recovery is demonstrated in the heating mode by expanding the normal expression for the coefficient of performance (COP) of an electrically-driven heat pump to an effective coefficient of performance (COP_{eff}). Letting Q_H denote heat pump heating capacity, Q_R equal recovered waste heat energy from the engine, and Q_F be engine fuel energy input, then

$$COP_{eff} = \frac{Q_H + Q_R}{Q_F} \quad (1)$$

Insight into the comparative performance of differently-powered heat pumps is obtained by expressing equation (1) in terms of component efficiencies and the engine heat recovery fraction. By defining the engine brake thermal efficiency (assuming no energy loss in the power train) as $\eta_t = HP/Q_F$, where HP is the mechanical energy input to the compressor, and by defining the fraction of engine fuel energy recovered as $\beta = Q_R/Q_F$, and the heat pump coefficient of performance as $COP = Q_H/HP$, equation (1) can be expressed as:

$$COP_{eff} = \eta_t \cdot COP + \beta \quad (2)$$

If the mechanical energy input to fans and miscellaneous equipment is denoted as HP' , then additional fuel energy equivalent to HP'/η_t must be considered, and equation (2) becomes:

$$\text{COP}_{\text{eff}} = \frac{\eta_t \cdot \text{COP} + \beta}{1 + \alpha} \quad (3)$$

where $\alpha = \text{HP}'/\text{HP}$ is the parasitic power fraction. In the cooling mode the waste heat is not normally utilized, and $\beta=0$. For an electrically-driven heat pump there is no waste heat recovery ($\beta=0$) and η_t denotes the efficiency of electrical power generation and transmission. The COP_{eff} then represents the efficiency of the heat pump based upon primary fuel (source) energy. The magnitude of the engine parameters (η_t, β) is essentially dependent on the type and design of the heat engine used (Stirling, Rankine, Brayton, Diesel, etc.), and proper matching of the engine with the heat pump unit. The heat pump COP is dependent on compressor and heat exchanger design, speed of operation, and the indoor-outdoor temperature limits over which the unit is required to operate.

The COP_{eff} of an engine-driven heat pump system is a valuable indicator of instantaneous efficiency at a particular indoor temperature, outdoor temperature, and compressor speed. It is not, however, a useful seasonal indicator because it doesn't account for the variation of building load, system capacity, and energy input with outdoor temperature, nor does it account for supplemental resistance heat which may be required at low temperatures. A meaningful index of seasonal efficiency is the seasonal performance factor (SPF) defined as:

$$\text{SPF} = \frac{\sum_{i=1}^I n_i \text{Load}(T_i)}{\sum_{i=1}^I n_i \left[\frac{\text{Load}(T_i)}{\text{COP}_{\text{eff}}(T_i)} \right]} \quad (4)$$

where n_i and T_i denote, respectively, the number of hours of operation in and the median temperature of the i th 5°F (2.78°C) increment, or bin, of the outdoor dry-bulb temperature range. The numerator is the total seasonal heating or cooling requirement, and the denominator is the total seasonal energy input.

This paper reports on experimental evaluation of an air-to-air, variable speed, engine-driven, 3-ton (10.5 kW) Rankine heat pump which was conducted at the National Bureau of Standards. Two series of tests were conducted. In the first, the power source was a water-cooled Stirling engine, and in the second, a single-cylinder water-cooled Diesel engine of similar horsepower was used. The specific objectives of the study were to experimentally determine the steady-state heating and cooling mode performance of both engine-driven systems as a function of outdoor temperature and compressor speed, and to determine and compare the seasonal performance of both systems. Beyond these specific objectives, however, the broader goal was to assess the concept of an engine-driven heat pump from an energy utilization viewpoint, and to establish some generalizations and design and operating guidelines for the use of thermal engines in heat pump applications.

DESCRIPTION OF EQUIPMENT AND INSTRUMENTATION

A Stirling engine is an external combustion engine which is well suited for buildings applications in that it is characterized by a potential for high thermodynamic efficiency, low exhaust emissions, quiet operation, and multi-fuel capability. Also, most of the waste energy is in the coolant. Its chief disadvantages are that it is still in the prototype stage and that its complexity and thermal design will probably dictate higher manufacturing costs than a conventional engine of comparable size, even under mass production conditions. In a buildings application, however, high engine cost may not be a serious disadvantage since equipment expenditures normally represent a small fraction of the overall building cost.

The engine selected for this study was a single-cylinder, 98 cm^3 (6 in^3) displacement, water-cooled engine whose maximum power was approximately 5 kW

(6.7 hp) at 3000 rpm. A description of the engine and its principles of operation are explained in detail in reference [8]. For measurements convenience, propane (C_3H_8) was used as the fuel in this study. Its flow rate was measured with a rotameter, and was thermostatically controlled so that a constant heater temperature of 608 °C (1126°F) was maintained. The combustion-air flow was measured with a rotameter, and was manually adjusted for an air-fuel mass ratio of 27 to 1 (72% excess air). Helium was used as the working fluid and was stored in external high pressure tanks. Power control was accomplished by manually admitting more helium to the engine cylinder or by venting excess helium to the atmosphere. Under field conditions, the helium circuit would be a closed loop with a pump and auto-controller. The energy rejected to the cooling water was determined by measuring the water flow rate through the engine and its corresponding temperature increase. The flow rate was manually adjusted in order to maintain a constant water outlet temperature of 60°C (140°F). This temperature was selected because it is sufficiently high for many space heating requirements. The coolant was circulated through a conventional automobile radiator and returned to the engine at a temperature typically between 43.3°C (110°F) and 48.9°C (120°F).

The Diesel engine was chosen such that its power and speed characteristics were generally comparable to the Stirling engine. It was a 4-stroke, single-cylinder, water-cooled, direct injection, 582 cm³ (36 in³) displacement engine, whose maximum power was approximately 6.5 kW (8.7 hp) at 2500 rpm. It was designed for marine applications and was equipped with a removable cylinder-head cooling jacket. The fuel consumption was determined by placing the fuel tank on an electronic scale and continuously recording its weight as a function of time. Combustion-air was delivered to the engine through a large volume surge tank which assured that the intake pressure fluctuations typical of a single-cylinder engine were damped out. The cooling water circuit was essentially equivalent to the one used for the Stirling engine. Engine outlet water temperature was maintained at 60°C (140°F) throughout the study, and the inlet temperature was typically 48.9°C (120°F).

The heat pump was a uniquely constructed apparatus whose major components were obtained from a commercial air-to-air heat pump. These components included the indoor and outdoor coil units, refrigerant lines, check and expansion valves, and the control unit. Since the compressor had to be externally powered, the hermetic compressor was replaced with a reciprocating, 4-cylinder, belt-driven, open compressor designed for Refrigerant 12. The outdoor coil and fan were placed inside a specially constructed insulated box which also contained three stages of electrical resistance "bucking" heat. The contained air was circulated around a loop and over these components. During the heating mode, low outdoor unit temperatures were achieved by the evaporator removing energy from the air. The "bucking" heaters were used to automatically control the desired temperature by supplying energy at a rate sufficient to balance the energy extracted by the evaporator. During the cooling mode, high outdoor temperatures were achieved by partially opening the outdoor unit, drawing in ambient air, and heating it with the resistance heaters to control its temperature to the desired level. The indoor unit consisted of a specially constructed L-shaped duct which contained the indoor A-frame coil and fan.

Heat pump instrumentation included thermocouples to measure the temperature of the refrigerant and air entering and exiting both coils. Also measured were compressor suction and discharge pressure and temperature, indoor coil pressure, refrigerant mass flow, and electrical input to the "bucking" heaters and to the indoor and outdoor fans. Thermocouple readings for both engine-driven heat pump systems were continuously recorded with either strip-chart recorders or with an automatic data acquisition system.

Figure 1 shows a general schematic diagram of either engine-driven heat pump system illustrating the major components. The entire system was located in a large environmental chamber which simulated indoor conditions by maintaining

a 21.1°C (70°F) and 50% relative humidity environment. The chamber had sufficient capacity to handle the heating and cooling loads imposed on it by the heat pump system. Figure 2 is a photograph of the Stirling engine and the indoor and outdoor units located in the chamber.

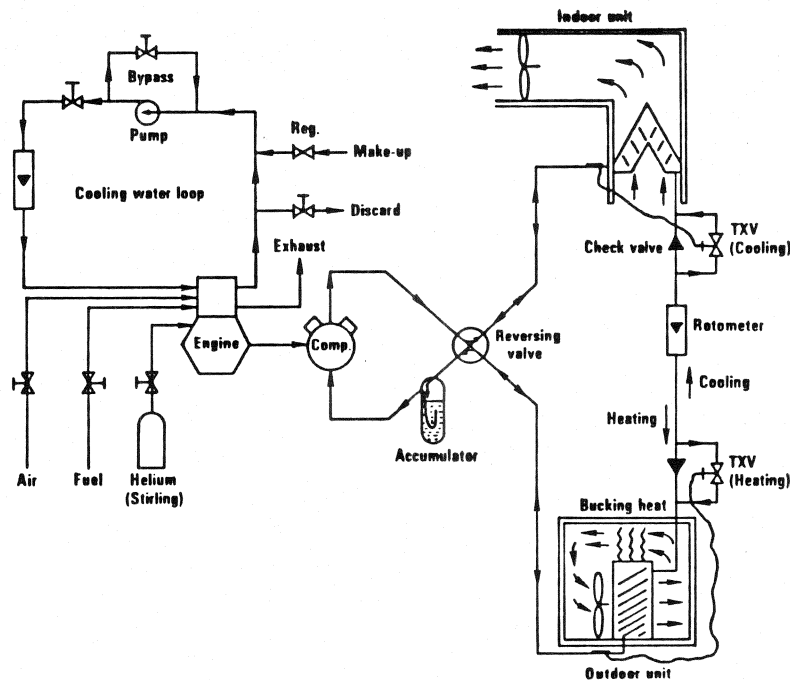


Figure 1. Schematic Diagram of Engine-Driven Heat Pump System

EXPERIMENTAL PROCEDURE

The experimental study was divided into several phases. One phase was devoted to determining the steady-state performance of the Stirling and Diesel engines over their respective speed and power ranges. An electric dynamometer was used during these tests and the speed and load were varied in small enough increments to produce smooth curves. Sufficient data was taken at each operating point to determine engine power (HP), brake specific fuel consumption, (bsfc; kg fuel consumed per kWh output), brake thermal efficiency (η_b), fuel energy (Q_F), and recovered waste energy (Q_R). Stirling engine data was taken from 1000-3000 rpm, and Diesel engine data was taken from 1000-2500 rpm.

Another phase was devoted to determining the steady-state performance of the heat pump in the heating and cooling modes as a function of outdoor dry-bulb temperature and compressor speed. The electric dynamometer was used as the power source during this phase. Outdoor temperatures ranged from -17.8°C (0°F) to 15.6°C (60°F) in the heating mode, and from 26.7°C (80°F) to 43.3°C (110°F) in the cooling mode. Compressor speeds varied from 900-1800 rpm. Sufficient data was recorded at each operating point to determine compressor power consumption, indoor coil capacity, fan power requirements, and heat pump coefficient of performance.

The steady-state performance of each engine-driven heat pump system was then analytically determined and experimentally verified as a function of outdoor

temperature and compressor speed by combining engine and heat pump performance characteristics. The analytical procedure and its experimental confirmation are discussed in reference [7]. The Stirling-to-compressor speed ratio was fixed at 1.41 and the Diesel-to-compressor speed ratio was 1.25. These ratios assured that the respective engine and compressor speed ranges were compatible.

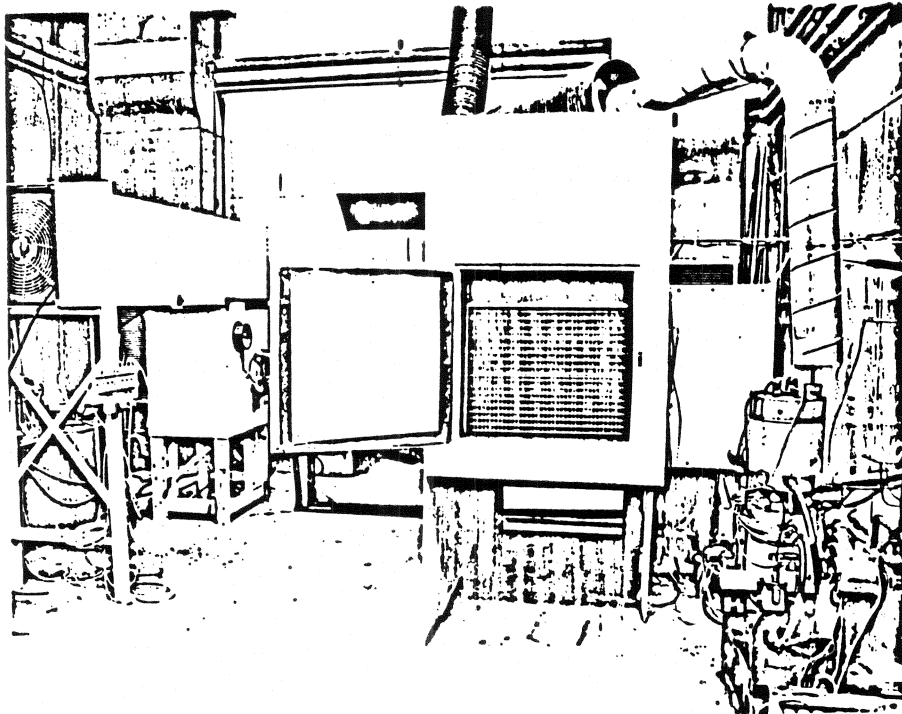


Figure 2. Stirling Engine and Indoor and Outdoor Units

EXPERIMENTAL RESULTS

Figure 3 illustrates a combined map of Diesel engine performance capability and compressor power requirement. The map relates engine brake power, brake specific fuel consumption, and engine speed. In addition, the heating mode power requirement of the compressor is presented as a function of outdoor dry-bulb temperature and engine speed. The engine power and fuel consumption have been adjusted to standard ambient conditions of 29.4°C (85°F) and 98 kPa (29 in. Hg) dry air.

The results indicate that at any given speed, specific fuel consumption is relatively high at low loads, but decreases as the load increases until a minimum is reached at approximately three-quarters load. Depending upon the speed, the corresponding optimum brake thermal efficiencies typically varied from 25-31%. The most efficient point of Diesel engine operation occurred at 3.73 kW (5 hp) and 1500 rpm, and the corresponding brake specific fuel consumption and thermal efficiency were 0.255 kg/kWh (0.42 lbm/hp-hr) and 31%, respectively. The corresponding heat pump operating point was at a compressor speed of 1200 rpm and an outdoor temperature of approximately 15.6°C (60°F).

It is apparent from Figure 3 that the Diesel engine is somewhat over-sized for this heat pump application in that the compressor power requirement does not generally cause the engine to operate in an efficient load-speed range. This is particularly true for low outdoor temperatures. Inclusion of indoor and outdoor fan power would tend to improve the matching between the engine and the

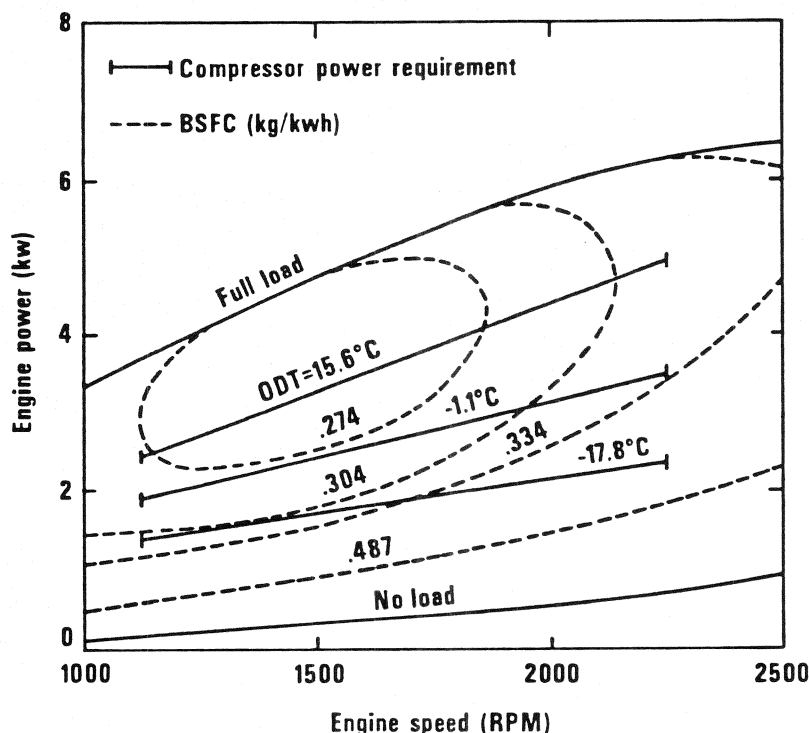


Figure 3. Diesel Engine-Compressor Performance Map
(Data corrected to 29.4°C and 98 kPa;
 $N_e/N_c = 1.25$)

heat pump. This was not done, however, because the increased power demand would have exceeded the power capability of the Stirling engine which was available, and it was felt that for comparison purposes it was necessary to retain the same operating basis for both engine-driven heat pump systems. If the engine and heat pump had been specifically designed as a unit, however, the heat pump total power requirement would have been more closely matched to the high efficiency region of the engine performance map. Because the COP of the engine-driven heat pump system is a function of engine efficiency η_t as well as fuel energy recovery fraction β , and because η_t and β are inversely proportional to each other, the system efficiency penalty stemming from oversizing is less significant than it might appear.

The Stirling engine-compressor performance map is illustrated in Figure 4 and is qualitatively similar to Figure 3. The Stirling's power capability is somewhat less than the Diesel's and it varies over a wider speed range. The most fuel efficient range of engine operation is 1500-1700 rpm, and the brake specific fuel consumption typically varies from 0.28-0.49 kg/kWh (0.46-0.8 lbm/hp-hr). The corresponding thermal efficiency variation is 28-16%, and could have been measurably increased by either raising the heater temperature above 608°C (1126°F) or by reducing the maximum coolant temperature below 60°C (140°F), or both. Since the heater temperature was fixed by the manufacturer and the coolant temperature was based upon space heating requirements, it was not feasible to change either limit. Figure 4 indicates that the Stirling engine and

compressor were slightly better matched than the Diesel engine-compressor in that the compressor required the Stirling to operate in a relatively more efficient load-speed range of its performance map for a wider range of compressor speeds and outdoor temperatures.

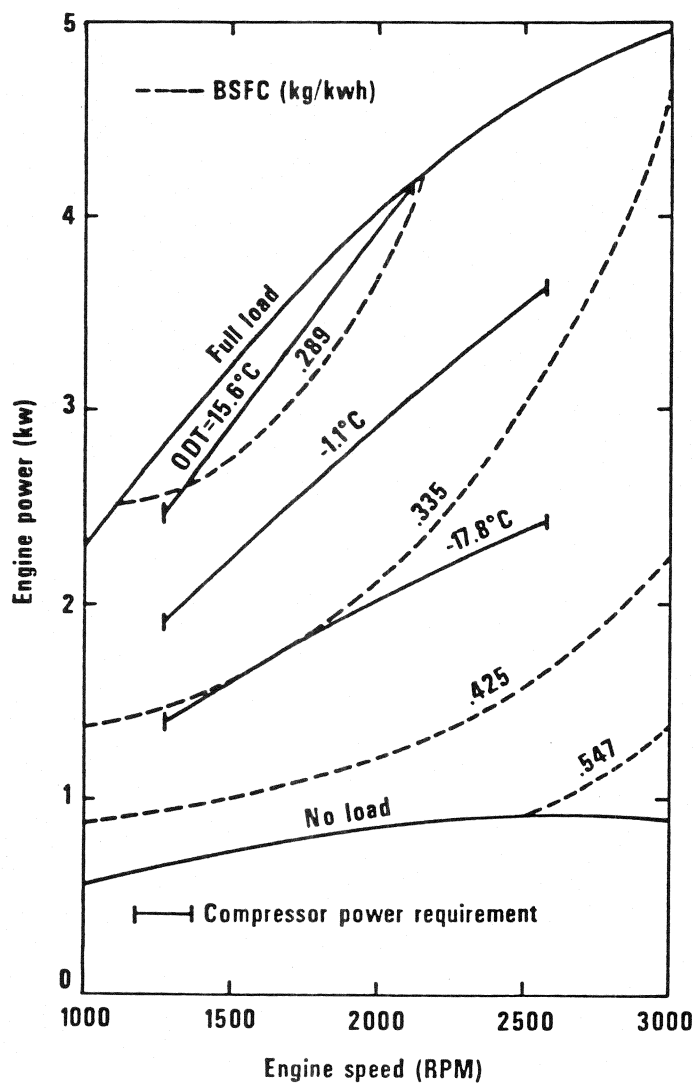


Figure 4. Stirling Engine-Compressor Performance Map (Heater Temperature = 608°C (1126°F), $N_e/N_c = 1.41$)

Figure 5 illustrates the variation of recovered waste energy expressed as a percentage of fuel energy input, and is presented as a function of engine power and speed for both engines. Although essentially all of the energy rejected to the coolant is recoverable, only part of the exhaust energy can be recovered because of the necessity of maintaining the exhaust gas at a high enough temperature to prevent condensation. Reference [9] indicates that the exhaust temperature leaving the heat recovery unit of a Diesel engine should not be less than $163 \pm 14^\circ\text{C}$ ($325 \pm 25^\circ\text{F}$). The energy recoverable from the Diesel engine exhaust was, therefore, determined from the gas mass flow rate and the enthalpy decrease between the measured exhaust temperature and the lower limit of 149°C (300°F). The exhaust gas specific heats were determined from data in Reference [10]. Since the Stirling combustion air preheater generally reduced the exhaust temperature below 232°C (450°F), and since the exhaust mass flow rate was generally moderate, it was determined that the recoverable exhaust energy from the Stirling was negligible relative to the coolant energy, and not economically recoverable. The energy rejected to the coolant of each engine was determined from the respective coolant mass flow rates and temperature increases.

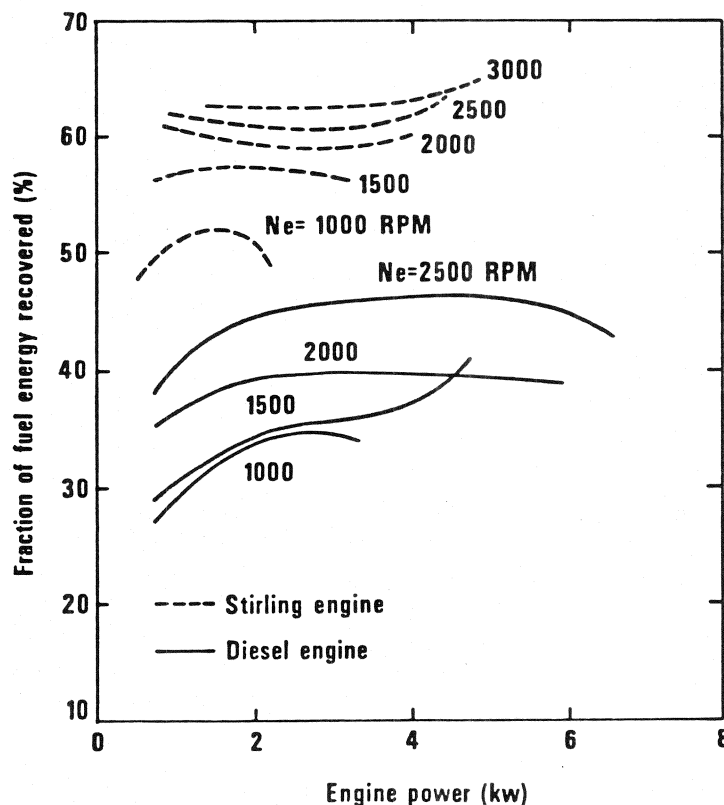


Figure 5. Percentage of Stirling Engine and Diesel Engine Fuel Energy Which is Recoverable

The results in Figure 5 indicate that, depending upon the speed and load, typically 50-60% of the Stirling engine's fuel energy may be recovered and used for space heating applications, whereas, only about 30-45% of the Diesel's fuel energy is recoverable. Of this, approximately 18-30% was in the coolant, and the remainder was recoverable from the exhaust. Reference [9] reports that typically 30% of a Diesel's full load fuel energy is rejected to the coolant, and approximately 17% is recoverable from the exhaust. The Stirling engine heat recovery data is consistent with data presented in Reference [11] where fuel energy recovery fractions of 46-54% were reported. The engine in that study was a 30 kW (45 hp) device using hydrogen as the working fluid, and it developed peak thermal efficiencies of approximately 32-38%, depending on the load. The heat recovery data of Figure 5 expressed as energy recovered per unit brake power is approximately 1179-2358 J/kW-sec (50-100 Btu/bhp-min) for the Diesel engine, and 1768-3537 J/kW-sec (75-150 Btu/bhp-min) for the Stirling. Therefore, at comparable speeds and loads, the total heat recovered from the Stirling engine was generally 50% greater than from the Diesel engine, and it was recovered entirely from the coolant. The rejection of large amounts of energy to an engine's coolant system might ordinarily be a disadvantage, particularly in closed systems where the high heat load must be rejected to the environment. However, in any heat recovery application where the heat can be usefully employed, such as in a heat pump system, it is an advantage. This is one of the attractive features of the Stirling engine for buildings applications.

A further comparison of Stirling and Diesel engine heat recovery is obtained by determining the fraction of the engine's rejected energy which is recoverable $\beta/(1-\eta_c)$. Analysis of heat recovery and thermal efficiency data showed that, depending upon the speed and load, typically 0.6-0.8 of the Stirling's rejected energy was recoverable, whereas, comparable values for the Diesel engine were only 0.4-0.6. Heat recovery data from Reference [12] indicates that these latter values are also approximately representative of large scale Diesel engines. In that study, approximately 0.43 of the fuel energy was recovered from a bank of five 600 kW (805 horsepower) Diesel engines in a total energy plant over a 12-month period. It should be emphasized at this point that the engine power, fuel consumption, and thermal data presented in Figures 3-5 are based upon a maximum coolant temperature of 60°C (140°F). The effect on engine performance and heat recovery of raising the coolant temperature is examined later in this paper.

Figure 6 illustrates the steady-state heating and cooling capacity of the Diesel engine-driven heat pump system as a function of outdoor temperature and compressor speed. The results are based upon an indoor temperature and relative humidity of 21.1°C (70°F) and 50%, respectively. Coil frosting during the heating mode did not occur because of the small amount of moisture in the air which was circulated in the outdoor unit. Heat pump capacity is superimposed to illustrate the effect of recovered engine heat in the heating mode. For clarity, the results have only been plotted for speeds of 900 and 1800 rpm. Capacity increases range from 30% at 900 rpm and 15.6°C (60°F) to 109% at 1800 rpm and -17.8°C (0°F). The results of the Stirling-driven heat pump system were qualitatively similar and are therefore not presented. However, the superior Stirling engine heat recovery caused corresponding capacity increases of 47-135%, respectively.

In order to assess the effects of capacity modulation on system performance, two typical residential energy loads were assumed. They are illustrated in Figure 6 as straight lines A and B, and are characterized by heat loss factors of 351 W/°C (666 Btu/hr-°F) and 527 W/°C (1000 Btu/hr-°F), respectively. Superposition of the system's capacity on these load curves results in fixed high-speed and low-speed balance points at -15.8°C (3.5°F) and -6.1°C (21°F), respectively, when operating against load A, and at -9.4°C (15°F) and -1.1°C (30°F) when operating against load B. The corresponding balance points of the Stirling system were -17.8°C (0°F) and -9.4°C (15°F), and -11.1°C (12°F) and -3.3°C (26°F). Therefore, depending upon the compressor speed and the building load, the superior

heat recovery characteristics of the Stirling engine generally resulted in a 1.7-3.3°C (3-6°F) decrease in the balance points relative to the Diesel-driven system.

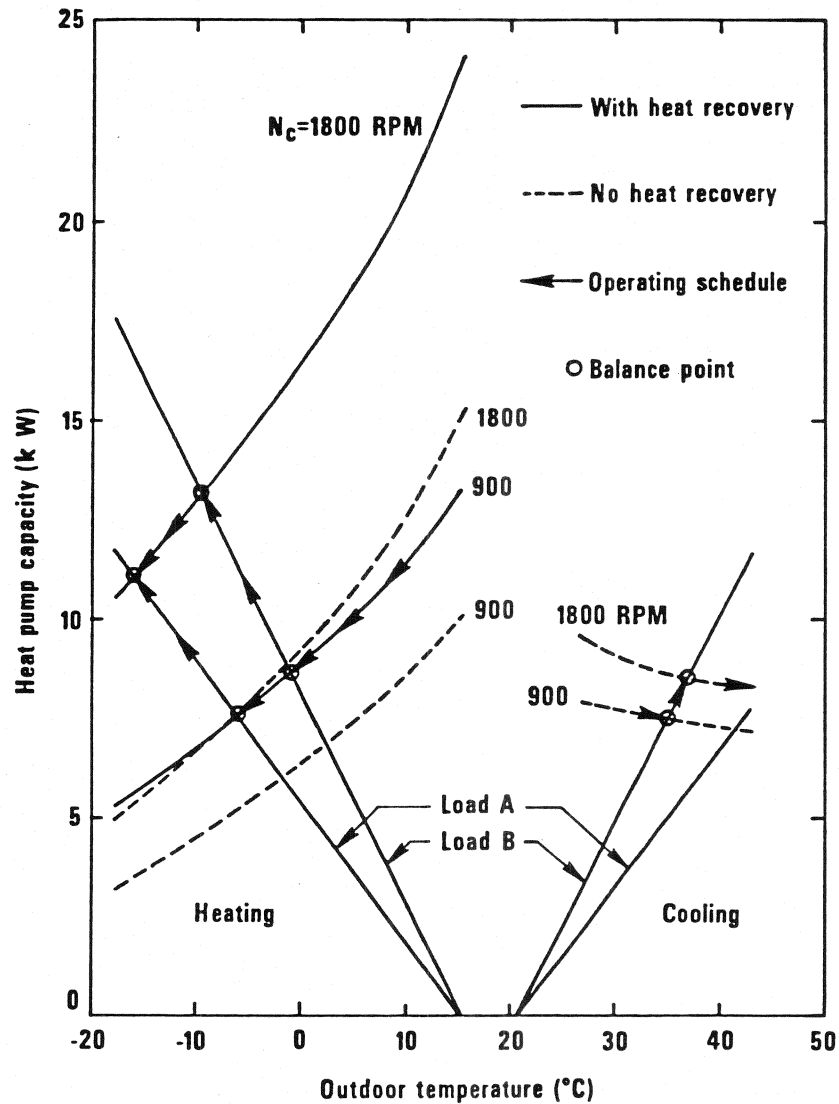


Figure 6. Diesel Engine-Driven Heat Pump System Heating and Cooling Capacity

Two variable-speed operating schedules, matched to loads A and B respectively, are shown in Figure 6 for the heating mode. A cooling mode operating schedule for load B is also shown. When operating in the heating mode at temperatures above the low-speed balance point, the compressor would be operated at

900 rpm and cycled on and off to meet the desired comfort conditions. At temperatures below the high-speed balance point, the compressor would operate continuously at 1800 rpm, but electric resistance heaters would be used to supplement the declining system capacity. When operating in a specified climate, the Stirling-driven system would require less resistance heat than the Diesel system because its high-speed balance point is lower.

The COP_{eff} of the Diesel-driven system is illustrated in Figure 7 for both operating modes as a function of outdoor temperature and compressor speed. The heating COP_{eff} was determined from equation (1), and the cooling COP_{eff} was equal to the ratio of indoor coil capacity to engine fuel energy. Indoor and outdoor fan power is not included in either mode. The relatively low heating COP_{eff} at 900 rpm is due to the low heat recovery fraction and low thermal efficiency of the diesel engine throughout the compressor power range at this speed (see Figures 3 and 5), relative to the same parameters at 1200 rpm.

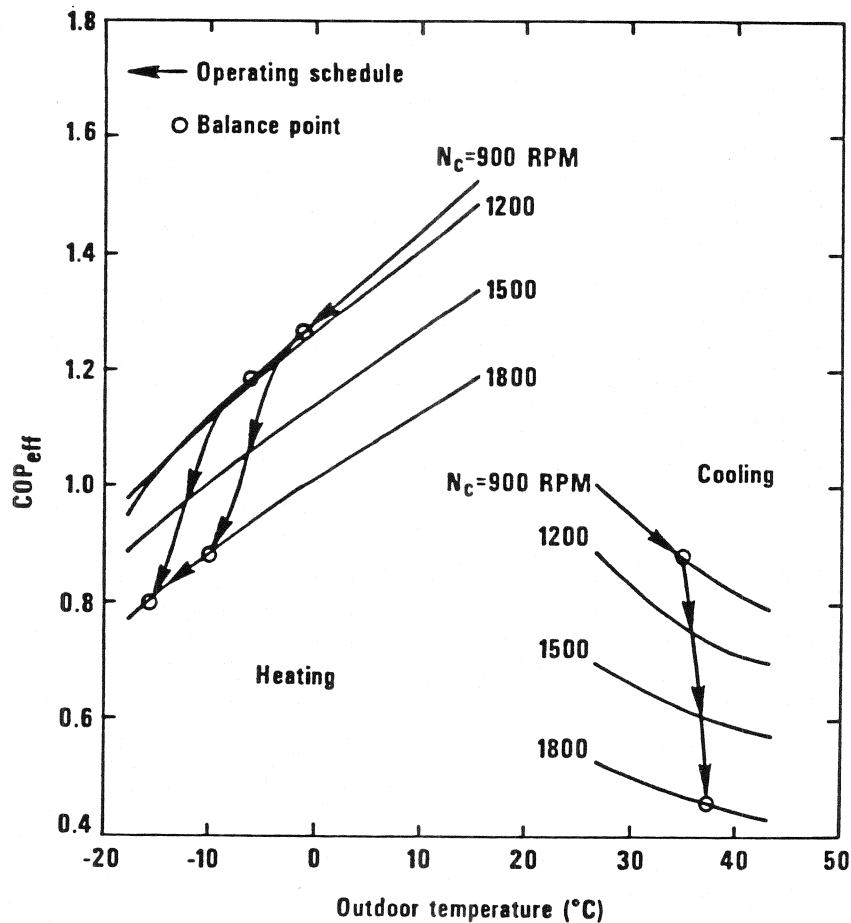


Figure 7. Diesel Engine-Driven Heat Pump System
Effective Coefficient of Performance

Figure 8 presents the Stirling-to-Diesel COP_{eff} ratio as a function of outdoor temperature and compressor speed. The heating COP_{eff} of the Stirling-driven

system is about 10-30% greater than the Diesel-driven system. These increases result from the greater Stirling engine heat recovery fraction at all speeds and loads illustrated in Figure 5. In the cooling mode, the COP_{eff} of the Stirling system is typically 90-98% of the Diesel system at most compressor speeds. This is because the Diesel thermal efficiency is often slightly higher than the Stirling efficiency at the loads imposed by the compressor. While the heating COP_{eff} ratios of Figure 8 pertain to the specific off-the-shelf hardware systems examined in this study, we feel that since they are dimensionless ratios, they are representative of the relative performance of specifically designed prototype Stirling-Diesel heat pump systems.

Equation (2) may be used to compare the COP_{eff} data of Figure 7 with the efficiency of the same heat pump unit when electrically-driven. Assuming that the efficiency of electrical power generation and transmission is 30% ($\eta_t = 0.3$), and noting that $\beta=0$ for an electric heat pump, then the equivalent heating COP_{eff} of the electric heat pump varies from 0.6-1.23. Therefore, the COP_{eff} of the Diesel-driven system with heat recovery is approximately 24-28% greater than the same heat pump when electrically-driven. A similar analysis shows that the Stirling system COP_{eff} is 34-73% greater than the electric heat pump.

The variable speed operating schedules of Figure 6 are illustrated in Figure 7 and indicate that when operating in the heating mode at temperatures above the low-speed balance point, the maximum efficiency occurs at the lowest compressor speed. At temperatures below this balance point, capacity modulation results in a COP_{eff} penalty. The conclusion is that capacity modulation should only be employed when operating at temperatures below the low-speed balance point, and that speed should only be increased sufficiently to meet the building load. An operating schedule is also shown for the cooling mode, and it indicates that a speed increase is required only when temperatures exceed the low-speed balance point.

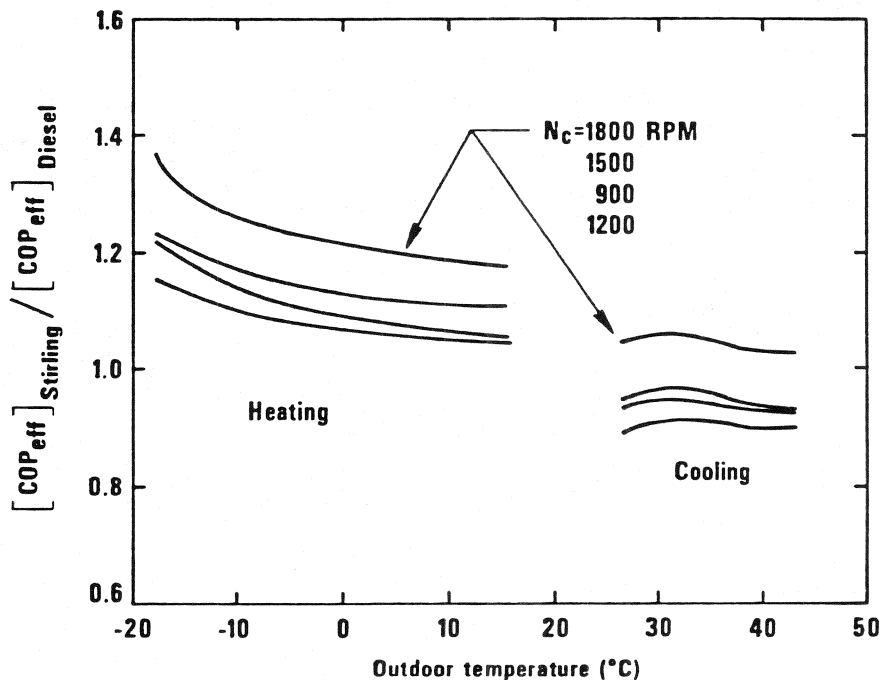


Figure 8. Stirling-to-Diesel Engine-Driven Heat Pump COP_{eff} Ratio

The impact of indoor and outdoor fan power on the heating COP_{eff} of either engine can be estimated by considering the approximate increase in fuel energy and system capacity resulting from the additional load on the engine. Total fan power data was taken during the testing program and was essentially constant at 0.82 kW (1.1 hp). Assuming that both engines have an average thermal efficiency of 25%, and that the recoverable portion of the Stirling and Diesel engine's fuel energy is 60% and 40%, respectively, then 1969 W (6720 Btu/hr) and 1312 W (4480 Btu/hr) of additional energy is recovered, and 3281 W (11200 Btu/hr) of additional fuel energy is required. Applying this data to equation (1) indicates that the COP_{eff} of both systems decreased by approximately 9-22%. The magnitude of the decrease was dependent primarily on the compressor speed, and the smallest decreases occurred at the highest speed where the heat pump capacity was the greatest.

SEASONAL PERFORMANCE FACTORS

In order to assess the seasonal efficiency of both engine-driven heat pump systems under different conditions, the heating SPF was calculated for each of three geographical areas. The areas chosen and their degree-days were Washington, D.C., (4244 DD), Chicago, Ill., (5882 DD), and Minneapolis, Minn., (8382 DD). The building heat loss, system capacity, fuel input to the system, and any required supplemental resistance heat were calculated for building loads A and B for each 2.78°C (5°F) increment, or bin [13], of the outdoor temperature range. This data was combined with U.S. weather information data on the number of hours per year that fall within each temperature increment for each city to determine the SPF. The SPF of the same heat pump when electrically-driven was also determined to illustrate the impact of engine heat recovery and capacity modulation. All electrical energy inputs were converted to equivalent source energy requirements with an assumed efficiency of electrical power generation and transmission of 30%. The results are presented in Table 1. The total seasonal heating requirement for the Washington, D.C. area was 17,700 kWh and 26,000 kWh for loads A and B, respectively. The corresponding heating requirement for the Chicago, Ill. area was 24,900 kWh and 37,300 kWh, and was 28,500 kWh and 42,800 kWh for the Minneapolis, Minn. area.

TABLE 1. SEASONAL PERFORMANCE FACTORS BASED UPON SOURCE ENERGY REQUIREMENTS

Power Source	Load A			Load B		
	Washington, D.C.	Chicago, Ill.	Minneapolis, Minn.	Washington, D.C.	Chicago, Ill.	Minneapolis, Minn.
Electric-driven, 1800 rpm	.76	.70	.63	.70	.62	.54
Diesel-driven, capacity modulated	1.29	1.21	1.13	1.30	1.01	.95
Stirling-driven capacity modulated	1.41	1.37	1.33	1.40	1.28	1.16

The data show that the SPF'S of the Diesel-driven system are about 70-86% greater than the electric heat pump, and that the SPF'S of the Stirling-driven system are about 85-115% greater than the electric heat pump. The result is that, because of recovered engine heat, engine-driven heat pumps require substantially less primary energy input than electric heat pumps during the heating season. The Diesel-driven system required 39-46% less energy input, and the Stirling-driven system required 46-53% less. A comparison of the Diesel and Stirling system data shows that the greater heat recovery of the Stirling engine results in approximately a 9-19% primary fuel savings relative to the Diesel system. The results also indicate that, regardless of the power source, a given size heat pump system becomes less efficient as the building load increases and as the climate becomes more severe. This is due to the increased requirement for supplemental resistance heat.

The reported seasonal efficiency and primary fuel savings are obviously restricted to the hardware configurations examined in this study and the climates selected. For the same climates, it's expected that the seasonal efficiency and fuel savings of prototype and production systems which are specifically designed and matched for heat pump-heat recovery applications would be somewhat greater than the values reported. Results from a theoretical off-design performance analysis [5] of a capacity-modulated heat pump driven by a hypothetical Stirling engine with a constant efficiency of 30% and 50% heat recovery, showed that the heating COP_{eff} varied from about 0.5-2.5 and that the SPF for the Chicago, Ill. area was 1.5. Results also predicted a 43.6 % energy savings relative to an electric heat pump.

DEFROST MODE ENERGY REQUIREMENTS

During a normal defrost cycle the heat pump is temporarily reversed and operated in the cooling mode until the ice on the outdoor coil is melted. The total energy required by the heat pump system during this period is an important consideration when evaluating the energy use of engine-driven heat pump systems. In addition to the fuel energy required by the engine during this period, supplemental electric resistance heat must also be supplied to help meet the building load and to replace the energy extracted from the building by the indoor coil. The total energy requirements during this brief but perhaps frequent defrost period can therefore become appreciable. The typical defrost energy requirement for residential applications can often be 5-10% of the heating season's energy input.

In order to compare the energy requirement of several modes of defrost operation, the total source energy required during a Stirling engine-driven normal defrost period with heat recovery was measured for several frosted-coil operating conditions. The source energy required by the electrically-driven heat pump during a normal defrost period was then measured under the same frosted-coil conditions. In addition, when the heat pump is engine-driven, it is also feasible that defrost be accomplished with recovered engine heat instead of heat pump reversal. The heat pump would be temporarily stopped; the engine would be operated under little or no load, and the recovered engine heat would be diverted across the outdoor coil to melt the ice. The total energy required during this period would be the electric resistance heat required to meet the building load plus the fuel energy required by the unloaded engine. It was initially thought that this total energy requirement might be less than during the normal defrost period. In order to evaluate this possibility, the total source energy consumption during such an "engine-heat" defrost period was measured. It was then compared with the source energy required during a Stirling-driven normal defrost with heat recovery, and an electrically-driven defrost with no heat recovery. As before, the efficiency of electric power generation and transmission was assumed to be 30%. For the range of operating conditions examined, the engine-driven defrost with heat recovery required less total total energy than either of the other two modes. The electric heat pump defrost required, on the average, approximately 34% more source energy than the

engine-driven defrost. This is because the indoor air must be tempered with electric resistance heat instead of available recovered engine heat. The "engine-heat" defrost mode required approximately 68% more energy than the normal engine-driven defrost, and this increase reflects the ineffectiveness of melting coil ice from the air side.

IMPACT OF COOLANT TEMPERATURE

The 60°C (140°F) coolant temperature used in this study was a compromise selection; it is sufficiently high for many residential space heating applications, and yet low enough to produce acceptable engine performance. However, for some heating applications a 60°C (140°F) coolant temperature is only marginally acceptable, and it's preferable to operate with higher temperatures. In order to determine the effect of a higher coolant temperature on η_c and β , and to estimate the impact on heat pump COP_{eff}, a series of Stirling and Diesel engine performance tests were conducted at a 102°C (215°F) coolant temperature.

The Stirling engine was performance tested at the higher coolant temperature over its entire speed and power range. The coolant circuit (Figure 1) was split into a high temperature primary circuit to cool the engine's head, and a low temperature secondary circuit to cool the engine's buffer zone and lubrication oil. For convenience, shop water at approximately 15°C (59°F) was used in the secondary circuit, and the energy rejected to this circuit was not included in the determination of β .

The Stirling engine results showed that a 42°C (75°F) increase in coolant temperature caused a reduction of brake power, thermal efficiency, and primary circuit energy recovery fraction at all speeds and loads. However, the qualitative variation was the same as before, and peak efficiencies at all loads still occurred at 1500-1700 rpm. The average full load engine power, efficiency, and recovery fraction decreased approximately 18%, 21%, and 17%, respectively, and these values are quantitatively representative of reductions throughout the entire speed-power range. Analysis of the data indicates that the decrease in Stirling engine efficiency results from rejecting energy to a higher mean temperature coolant. Analysis also showed that when the heat rejected to the secondary coolant circuit was considered, the total heat recovery fraction was generally equal to or greater than the previous results. There was a small increase in the exhaust energy, but the recoverable portion was still small relative to the coolant energy, and not economically recoverable.

The Diesel engine was tested over the entire load range at its optimum speed of 1500 rpm ($N_c = 1200$ rpm). The results showed that full load power increased approximately 5%, and that changes in η_c and β averaged about +5% and -7%, respectively. Analysis showed that the fraction of fuel energy rejected to the Diesel coolant decreased by about 25% because of the decreased temperature difference across the cylinder walls. The major portion of this diverted energy appeared in increased partially-recoverable exhaust energy and increased nonrecoverable radiation and convection losses. The remainder was indirectly converted into useful work as a result of decreased frictional effects at the elevated lubrication oil temperatures. It's believed that the increase in brake power and η_c found in this instance essentially reflects an increase in lubrication oil temperature and thus a decrease in viscosity. It's expected that in larger Diesel engines, lubrication oil coolers would be maintained at a design temperature; frictional effects would remain the same and thermal efficiency would be essentially unchanged. Therefore, most of the energy diverted from the coolant would appear either in the lubrication oil or in the exhaust. In both cases it would be partially-recoverable.

The most realistic way to judge the effect of an increase in coolant temperature is when the engine is required to provide the same power before and after the temperature change. Accordingly, it was determined that when the Stirling engine powered the heat pump at $N_c = 1200$ rpm ($N_e = 1700$ rpm) throughout

the outdoor temperature and compressor power range illustrated in Figure 4, the average reductions in η_t and β were approximately 19% and 18%, respectively, resulting in an average decrease in COP_{eff} of 19%. However, since the decrease in heat recovery fraction was less than the decrease in thermal efficiency, there was actually about 2% more recoverable energy in the coolant at the higher coolant temperature than at the lower temperature. Even though the coolant energy increased somewhat, the increased fuel energy required to meet the same load caused a net decrease in COP_{eff} , as predicted from equation (1).

When the Diesel engine powered the heat pump throughout the compressor power range at $N_c = 1200$ rpm (Figure 3), the changes in η_t , β and COP_{eff} averaged approximately +2.5%, -12%, and -5%, respectively. As noted before, the increase in η_t is probably a result of lube oil viscosity decrease, and may not be the sort of condition the engine could actually run under for an extended period. Therefore, the efficiency increase should be discounted.

A generalization of these results is that an increase in mean coolant temperature will cause a decrease in the COP_{eff} of both heat pump systems. As the coolant temperature of either engine increases, β decreases because an increasing portion of the "waste" energy is shifted to non-recoverable jacket losses and partially-recoverable exhaust energy.

SUMMARY

Overall results of the study indicate that: (a) recovered engine heat produces substantial increases in heating capacity and COP_{eff} , regardless of the power source, (b) capacity modulation at temperatures between the high- and low-speed balance points results in a closer match between heat pump capacity and building load, thereby reducing cycling and increasing instantaneous and seasonal efficiencies, (c) engine-driven heat pump systems require substantially less primary fuel energy than electric heat pumps during the heating season, (d) less primary source energy is required during a defrost cycle by an engine-driven heat pump than by an electric heat pump, (e) an engine-driven system using recovered engine heat to defrost the coil from the air side is less effective than the usual reverse cycle method, (f) the Stirling engine-driven heat pump system was characterized by greater heat recovery, heating capacity, COP_{eff} , and lower primary fuel energy than the Diesel-driven system, (g) the SPF of the Stirling-driven heat pump was greater than either the Diesel-driven or the electric heat pump, and (h) an increase in coolant temperature causes a COP_{eff} decrease for both systems because of adverse heat recovery effects, with the greatest penalty suffered by the Stirling engine.

The overall performance of an engine-driven heat pump system is a function of heat pump COP, engine efficiency, engine waste heat recovery fraction, building load, defrost means, and the climate in which the system operates. When comparing the total energy utilization of two or more prime movers, it is important to consider both the thermal efficiency and the engine's heat recovery. When expressed as either a fraction of fuel energy input or as energy recovered per unit power output, the total heat recovery of the Stirling engine was generally 50% greater than the Diesel engine, regardless of the speed or load. While this margin might shift downward somewhat as a result of design modifications to the Diesel engine and thermal efficiency improvements in the Stirling engine, it would still be significant enough to favor the Stirling engine as the prime mover in most heat recovery applications.

The purpose of this study was to obtain only a thermodynamic evaluation of the engine-driven heat pump as applied to buildings. The evaluation was based on the use of off-the-shelf components matched for size but not optimized for performance. Therefore, the results shown could be useful for estimating the potential of engine-driven heat pump systems, but certainly do not constitute a limit. That is, any system designed specifically for a given application could likely yield a higher thermal effectiveness than these results indicate. Counteracting this optimism, however, are various economic tradeoffs. The development

of a prime mover that would have the operating life required for buildings application would appear to be extremely expensive. The mechanical complexity of such a system would surely require more frequent, more highly skilled and thus more expensive maintenance procedures compared to existing systems. Although it is virtually certain that all energy costs will continue to rise, the relative costs between oil, gas and electricity are not clear for the future, making marginal payback period predictions difficult. Thus, the implementation of these systems would still appear to be a highly speculative venture requiring extensive life-cycle-cost analysis as the ultimate determination.

ACKNOWLEDGEMENTS

The authors would like to express their appreciation to Mr. David Ward for his help during the experimental phase of this project. We would also like to thank the Philips Research Laboratories of Eindhoven, Netherlands for providing the Stirling engine which was used during this study.

REFERENCES

1. Gordian Associates, Inc., "Heat Pump Technology," Report Prepared for the U.S. Department of Energy, Dec. 1977, pp. 72-93.
2. Auxer, W. L., "Development of a Stirling Engine Powered Heat Activated Heat Pump," Proceedings of the 12th Intersociety Energy Conversion Engineering Conference, Washington, D.C., Sept. 1977, pp. 397-401.
3. Friedman, D., "Light Commercial Brayton/Rankine Space Conditioning System," Proceedings of the 12th Intersociety Energy Conversion Engineering Conference, Washington, D.C., Sept. 1977, pp. 172-178.
4. Swenson, P. F., and Rose, R. K., "Development of the High Seasonal Performance Factor Gas Heat Pump," Proceedings of the 12th Intersociety Energy Conversion Engineering Conference, Washington, D.C., Sept. 1977, pp. 390-396.
5. Wurm, J., and Panikker, G. P. K., "Evaluation of Engine-Driven Heat Pump Systems of Small Capacities," presented at Environment and Energy Conservation Symposium of the EPA and the ERDA, Denver, Colorado, Nov. 1975.
6. Sarkes, L. A., Nicholls, J. A., and Menzer, M. S., "Gas-Fired Heat Pumps: An Emerging Technology," ASHRAE Journal, Mar. 1977, pp. 36-41.
7. Didion, D. A., Maxwell, B. R., and Ward, D., "A Laboratory Investigation of a Stirling Engine Driven Heat Pump," Proceedings of Energy Conservation in Heating, Cooling and Ventilation of Buildings: Heat and Mass Transfer Techniques and Alternatives, Dubrovnik, Yugoslavia, Sept. 1977, Hemisphere Press.
8. Walker, S., Stirling Cycle Machines, Clarendon Press, Oxford, England, 1973.
9. Caterpillar Tractor Co., Total Energy Handbook, 1969.
10. Boyen, J. L., Practical Heat Recovery, John Wiley and Sons, Inc., 1975.
11. Meijer, R.L., "The Philips Stirling Thermal Engine," Thesis, Technische Hogeschool Delft, Nov. 1960, pp. 95-101.
12. Hebrank, J., et. al., Performance Analysis of the Jersey City Total Energy Site: Interim Report, National Bureau of Standards, Washington, D.C., NBSIR 77-1243, July 1977.
13. ASHRAE Handbook, 1976 Systems Volume, Chapter 43.